Detection of Antigen−Antibody Binding Events with the Atomic Force Microscope†

Stephanie Allen,*,‡ Xinyong Chen,‡ John Davies,§ Martyn C. Davies,‡ Adrian C. Dawkes,§ John C. Edwards,§ Clive J. Roberts,‡ Joanna Sefton,§ Saul J. B. Tendler,‡ and Philip M. Williams‡

Laboratory of Biophysics and Surface Analysis, Department of Pharmaceutical Sciences, The University of Nottingham, University Park, Nottingham NG7 2RD, U.K., and Johnson & Johnson Clinical Diagnostics, Pollards Wood Laboratories, Nightingales Lane, Chalfont St. Giles, Buckinghamshire HP8 4SP, U.K.

Received October 8, 1996; Revised Manuscript Received March 25, 1997⊗

ABSTRACT: An atomic force microscope (AFM) has been used to directly monitor specific interactions between antibodies and antigens employed in an immunoassay system. Results were achieved using AFM probes functionalized with ferritin, and monitoring the adhesive forces between the probe and anti-ferritin antibody-coated substrates. Analysis of the force distribution data suggests a quantization of the forces, with a period of 49 ± 10 pN. This periodic force may be attributed to single unbinding events between individual antigen and antibody molecules. These results demonstrate that the AFM could be employed as an analytical tool to study the interactions between the molecules involved in biosensor systems. The potential of the technique to provide information relating to the manner in which the antibody molecule binds to its specific antigen is also discussed.

The ability of the atomic force microscope (AFM)[1] (Binnig et al., 1986) to directly measure discrete intermolecular forces of 10 pN or less was first highlighted by Hoh et al. (1993). Various groups have exploited this application of the instrument and were able to quantify the forces required to separate individual receptor−ligand molecules (Boland et al., 1995; Dammer et al., 1995, 1996; Florin et al., 1994; Lee et al., 1994a,b; Ludwig et al., 1994; Moy et al., 1994a,b). Here we provide conclusive evidence that the AFM can be employed to quantify the force required to unbind individual protein molecules, specifically in an antibody−antigen system. Importantly we demonstrate this ability with a molecular system employed in an immunoassay format.

The interaction between an antigen and antibody is fundamental to many immunochemical techniques. Perhaps the most powerful of these techniques is the immunoassay (Harlow & Lane, 1988b; Hage, 1993), which can be used to detect a wide range of antigens or antibodies present in fluids in a quantitative or qualitative manner. In previous work the imaging abilities of the AFM have been used to study the ferritin binding capacity of immunoassay well surfaces employing different antibody immobilization techniques (Davies et al., 1994). The AFM has also been used to distinguish between classes of antibody deposited on the immunoassay surface (Roberts et al., 1995, 1996).

X-ray crystallographic studies of the complexes between specific antibodies and antigens have revealed that antibody−antigen interactions involve van der Waals interactions, the formation of hydrogen bonds, and, to a lesser extent, the formation of salt-bridges (Braden & Poljak, 1995). The relative strength of the antibody−antigen interaction is estimated using their affinity constants (Harlow & Lane, 1988a) which can be determined experimentally by immunoassay (Chu et al., 1995), fluorescence methods (Bruggeman et al., 1995), and surface plasmon resonance (Pellequer & Vanregenmortel, 1993). However, none of these methods can be used to directly measure the strength of the antigen−antibody bond.

The forces which control the interactions between anti-fluorescyl antibody fragments and fluorescein molecules supported in planar bilayers were characterized using the surface forces apparatus (Leckband et al., 1995). It was shown that long-range electrostatic forces effectively steer the antigen toward the binding site on the antibody. The forces controlling the interactions between surfaces functionalized with antigens and antibody have also been studied by total internal reflection microscopy (Leibert & Preive, 1995) and radial fluid flow chamber assay (Kuo & Lauffenburger, 1993).

Recently Stuart et al. (1995) used the AFM to investigate the specific interaction between an antifluorescyl antibody-functionalized surface and fluoresceinated silica beads. Another group (Hinterdorfer et al., 1996) attached polyclonal anti-human serum albumin antibodies (anti-HSA) to an AFM probe by means of a flexible poly(ethylene glycol) (PEG) spacer group and observed interactions between the probe and surface-bound antigen. Interactions between polyclonal antibiotin antibodies and biotinylated AFM probes have also been observed (Dammer et al., 1996).

In the case of AFM force experiments, the conformational changes which proteins may undergo during their adsorption to surfaces (Hollander et al., 1986) may lead to a reduction in the number of sites at which the receptor−ligand complex can form. Ferritin is an iron storage protein composed of 24 homologous subunits arranged in a spherical shell-like

† This work was funded by an EPSRC CASE award with Johnson & Johnson Clinical Diagnostics, the EPSRC Nanotechnology Initiative, and an EPSRC/ DTI Nanotechnology LINK Scheme in collaboration with Kodak Limited, Oxford Molecular Group plc, and Fisons Instruments plc.

* Address correspondence to this author. Tel: +44-(0)115 951 5063. FAX: +44-(0)115 951 5110.

‡ The University of Nottingham.

§ Johnson & Johnson Clinical Diagnostics.

⊗ Abstract published in *Advance ACS Abstracts,* May 15, 1997.

[1] Abbreviations: AFM, atomic force microscope; BSA, bovine serum albumin; PEG, poly(ethylene glycol); anti-HSA, anti-human serum albumin antibody; HSA, human serum albumin.

S0006-2960(96)02531-7 CCC: $14.00

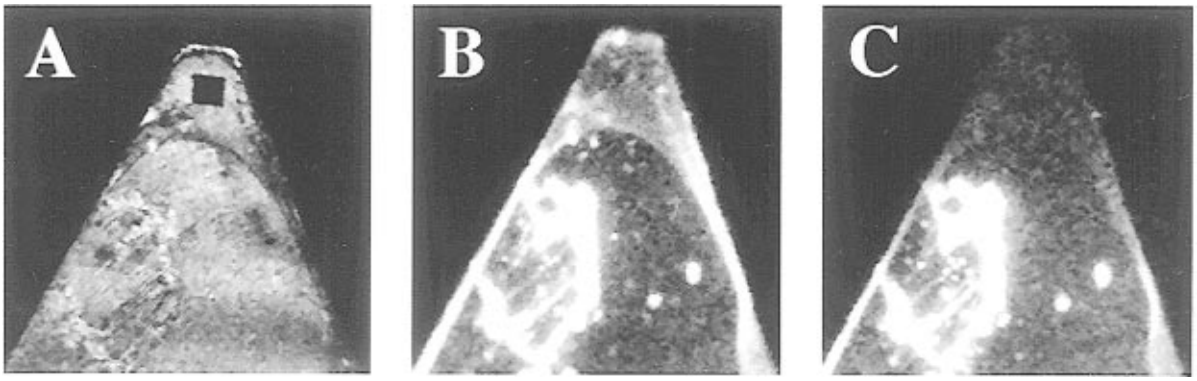

FIGURE 1: Series of images of an AFM cantilever and probe functionalized with fluorescein-labeled antibody, obtained with a confocal scanning laser microscope. (A) Reflectance image, to aid localization of the AFM probe (black square); (B) fluorescence image of the cantilever after antibody immobilization; and (C), as in B, but after photobleaching the end portion of the cantilever. The reduction in signal in the bleached area confirmed that the fluorescence signal was attributable to the labeled antibody and not to the probe or cantilever itself.

manner (Harrison et al., 1989). Each ferritin molecule contains, therefore, many identical antibody binding sites or epitopes. Due to its polyepitopic nature, the availability of antibody binding sites is less dependent on the conformation/orientation of the ferritin molecule on the probe surface.

In this paper the adhesive forces between ferritin-functionalized AFM probes and anti-ferritin antibody-coated silicon substrates are measured. Polystyrene microtiter well surfaces functionalized with anti-ferritin antibody provide the analyte capture component of an AMERLITE immunoassay, which can be employed to detect serum ferritin levels. Results are presented which demonstrate that the AFM could be employed as an analytical tool to study the interactions between the molecules involved in biosensor systems. The polyepitopic nature of the ferritin molecule also allows the binding of more than one antibody molecule to each molecule of ferritin, so increasing the chance of observing multiple binding events in force measurements. The observation of such force curves allows us to discuss the potential of the technique to provide information relating to the manner in which the antibody molecule binds to its specific antigen.

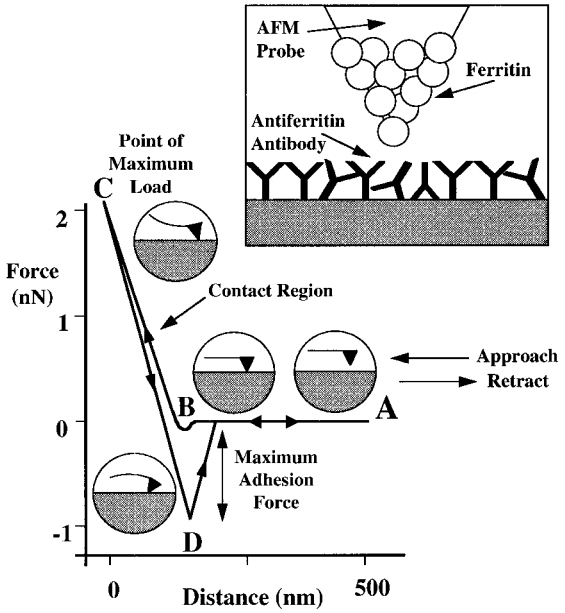

FIGURE 2: During a force measurement cycle the probe is moved toward the surface (approach trace) at constant velocity until it is brought into contact with the sample (B) until a predetermined point of maximum load is reached (C). The direction of motion is then reversed, and the probe is withdrawn from the sample surface. A plot of cantilever deflection against distance moved by the fixed end of the cantilever is obtained as raw data. As the probe is withdrawn from the sample (retract trace) the probe "sticks" to the surface due to interactions between the probe and the sample (D). The magnitude of this "sticking" force is calculated from the difference between the maximum cantilever deflection during the withdrawal phase of the cycle and the point of zero cantilever deflection.

MATERIALS AND METHODS

Sample Preparation. Anti-ferritin mouse monoclonal IgG2a (Johnson & Johnson Clinical Diagnostics, Chalfont St. Giles, Buckinghamshire, U.K.) was purified from mouse ascites fluid by protein A chromatography. The purity of the antibody preparation was confirmed using SDS−polyacrylamide gel electrophoresis (data not shown). Purified anti-ferritin antibody was immobilized onto polished silicon wafers using a method adapted from Vincker et al. (1995). Proteins were covalently attached to the substrate (and probe) surfaces in these experiments to ensure that the molecules were not pulled away from the surfaces during force measurements. For example, it has been reported that the force required to break a C−C covalent bond is at least 10 nN (Dammer et al., 1995), which is 5 times larger than the largest force measured in these experiments.

Silicon wafers were cleaned by sonication in a series of solvents (chloroform, isopropyl alcohol, methanol, and then water). The surfaces of the wafers were then oxidized using an oxygen plasma (200 W, 1 min), after which they were immediately transferred to a 1.5% v/v solution of 3-aminopropyldimethylethoxysilane in toluene. After 2 h the silanized substrates were sonicated in the series of solvents to remove any unbound silane. The amino-functionalized substrates were then activated by incubating the silanized wafers in a 10% v/v solution of glutaraldehyde (Grade II, 25% in aqueous solution) in potassium phosphate buffer (100 mM, pH 7) for 1 h at room temperature. After the wafers were rinsed thoroughly with deionized water to remove any unreacted glutaraldehyde, the antibody solution (0.9 mg mL^{-1} in phosphate buffer) was dropped onto the surface of each wafer and incubated at room temperature for 1 h. After this time the wafers were thoroughly rinsed with deionized water and buffer to remove any loosely bound biological material. Wafers were stored in phosphate buffer, at 4 °C, until used. X-ray photoelectron spectroscopy analysis of each surface

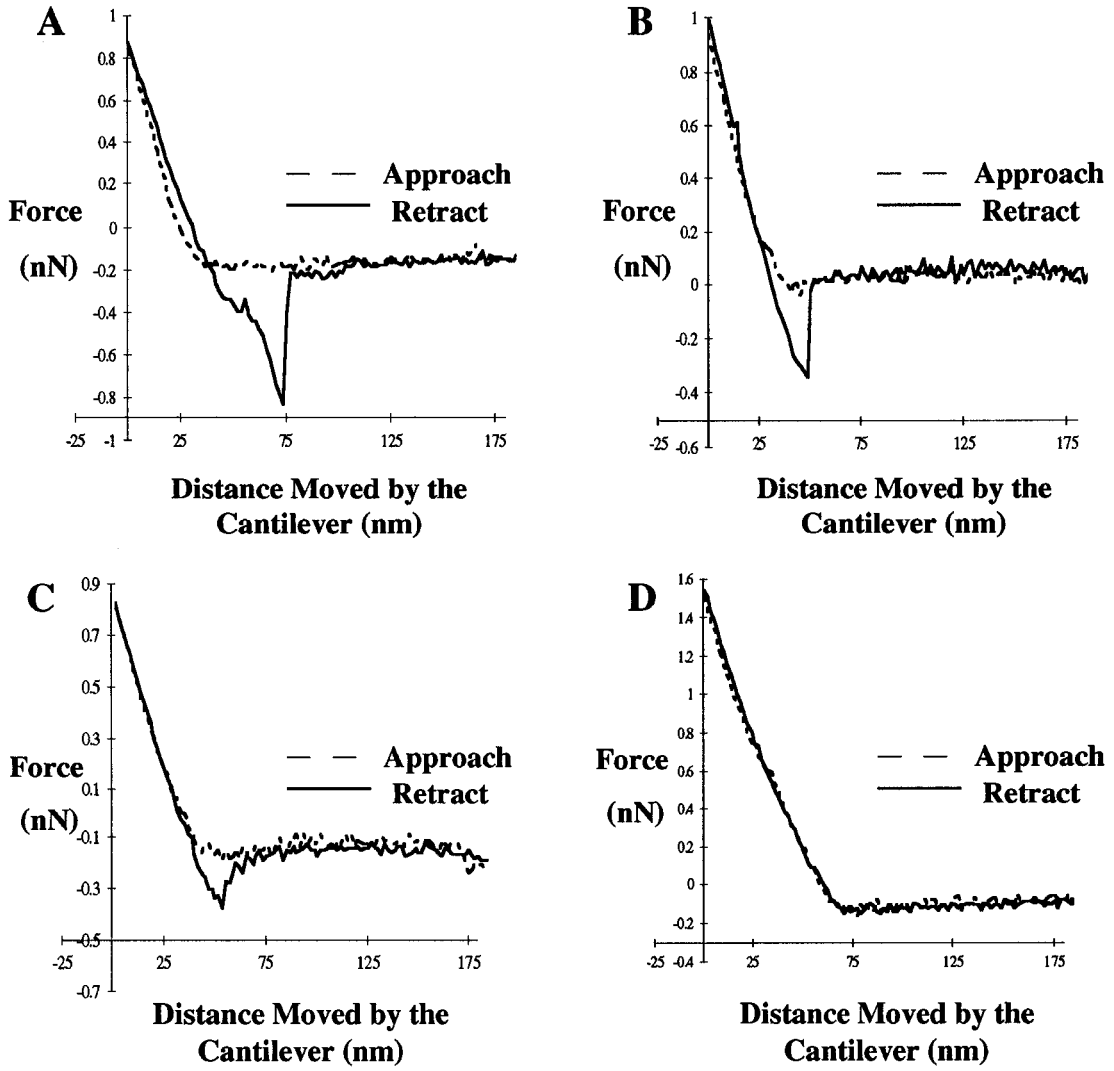

FIGURE 3: Force measurement between a silicon substrate coated with anti-HSA antibody and (A) a clean silicon nitride probe, (B) an amino-terminated probe after silanization, (C) an aldehyde-activated probe after treatment with glutaraldehyde, and (D) a ferritin-coated probe.

after the last stage in the immobilization process confirmed the presence of protein on the surface of the silicon wafer.

Probe Functionalization. Cantilevers (Topometrix Corporation, Saffron Walden, Essex, U.K.) with silicon nitride (Si_3N_4) probes were functionalized with human spleen ferritin (Johnson & Johnson Clinical Diagnostics, Chalfont St. Giles, Buckinghamshire) using the immobilization protocol outlined above. Probes were cleaned/oxidized prior to protein immobilization using an oxygen plasma (10 W, 30 s). After the surface of silanized probes was activated with glutaraldehyde, they were incubated in a solution of ferritin (0.15 mg mL^{-1} in phosphate buffer) for 1 h. The probes were then rinsed with deionized water and buffer to remove loosely bound ferritin and stored in buffer, at 4 °C, until used. A probe was derivatized with fluorescein-labeled antibody (Calbiochem, Nottingham, U.K.) and analyzed using a Bio-Rad MRC-600 confocal scanning laser microscope (Shotton, 1993; see Figure 1). The detection of fluorescence from the probe surface after the immobilization of the antibody confirmed the efficacy of the immobilization process. Confocal images were analyzed and processed where necessary using the Genesis Graphics System (Williams et al., 1991).

AFM Analysis. Force measurements were recorded using a Topometrix Explorer AFM (Topometrix Corporation, Saffron Walden, Essex, U.K.). Experiments were performed in freshly prepared potassium phosphate buffer (100 mM, pH 7) in a glass liquid cell which was cleaned thoroughly prior to use. Force measurements were obtained between ferritin-functionalized AFM probes and silicon wafers to which anti-ferritin antibody had been immobilized. To confirm the presence of specific ferritin binding, ferritin binding sites on the antibody-functionalized surface were blocked by flooding the experimental system with ferritin (0.15 mg mL^{-1}). After 1 h the AFM liquid cell was rinsed thoroughly with potassium phosphate buffer to remove excess ferritin. Force measurements were then obtained between the derivatized probe and the blocked surface. Additional force measurements were also recorded between ferritin-derivatized probes and wafers coated with anti-HSA as a control experiment. The spring constants (k) of individual cantilevers were determined using the resonant frequency method outlined by Cleveland et al. (1993) and were found to be within the range 0.043−0.057 Nm^{-1}.

RESULTS AND DISCUSSION

The AFM cantilever and probe system can be used as an ultrasensitive force apparatus which is capable of detecting the forces required to separate individual receptor−ligand

interactions. The study outlined in this paper employs a method previously described by ourselves (Allen et al., 1996) and other groups (Butt et al., 1995; Lee et al., 1994a,b; Moy et al., 1994a,b). A schematic diagram of the interaction between a ferritin-functionalized probe and an antibody-coated silicon wafer is shown in Figure 2. The maximum cantilever deflection during the retract phase of the force measurement is related directly to the magnitude of the force required to break the antigen−antibody bond(s) formed on contact. Recently, Grubmüller et al. (1996) stated that separation forces measured in such AFM experiments represent "the largest force along the actual unbinding reaction pathway, and is given by the steepest slope in the free energy profile along that pathway." In these experiments the cantilever deflection was converted into the force experienced by the AFM probe as follows: the deflection signal, measured in nanoamperes (nA), was first converted to a deflection distance (nm) using the gradient of the linear portion of the retract trace (nA nm^{-1}) in the contact region of the force curve. This distance was then converted to a force value (nanonewtons, nN) using the experimentally determined cantilever spring constant (k) and Hookes law ($F = -kd$).

When the forces required to separate receptor−ligand interactions are measured, it is essential to perform control experiments to ensure that the measurements correspond to the specific receptor−ligand interaction and not to other nonspecific sources (Dammer et al., 1996). For example, Lee et al. (1994) and Allen et al. (1996) coated both probes and substrates with monolayers of bovine serum albumin (BSA) and established that force measurements between such surfaces displayed no specific or nonspecific interactions. In those experiments the BSA-coated surfaces provided a suitable background substrate to which the receptor or ligand molecules could then be immobilized. The covalent immobilization strategy employed here has allowed a more direct approach to the discrimination of specific and nonspecific forces. This was achieved by characterizing forces between an anti-HSA-coated silicon wafer and (i) a clean silicon nitride probe (Figure 3A), (ii) an amino-terminated probe after silanization (Figure 3B), (iii) an aldehyde-activated probe following glutaraldehyde treatment (Figure 3C), and (iv) a ferritin-coated probe (Figure 3D), and an anti-ferritin antibody-coated silicon wafer and a ferritin-coated probe (see Figure 4). In these experiments the anti-HSA-functionalized substrate was employed as a control surface which was not expected to specifically interact with ferritin functionalized probes.

The force−distance curves between the anti-HSA-coated surface and the probe before ferritin immobilization (Figure 3A−C) reveal a significant level of adhesion which would mask specific interactions. However, following ferritin immobilization (Figure 3D) the force measurements displayed no adhesive forces above the background noise level. This confirmed that there was no specific interaction between the anti-HSA antibody and the ferritin and that the immobilized protein layers prevent nonspecific interactions between the surface chemistries of the probe and the substrate.

Figure 4A displays a typical force measurement between a ferritin-coated probe and an anti-ferritin antibody-functionalized surface. A sharp adhesion point is observed in the retract phase of the measurement. To confirm that the antigen−antibody interaction was causing the observed discontinuities in the force curves the experimental system was flooded with excess antigen so that surface antigen binding sites were occupied. Figure 4B shows that discrete adhesion points were not observed for such a system.

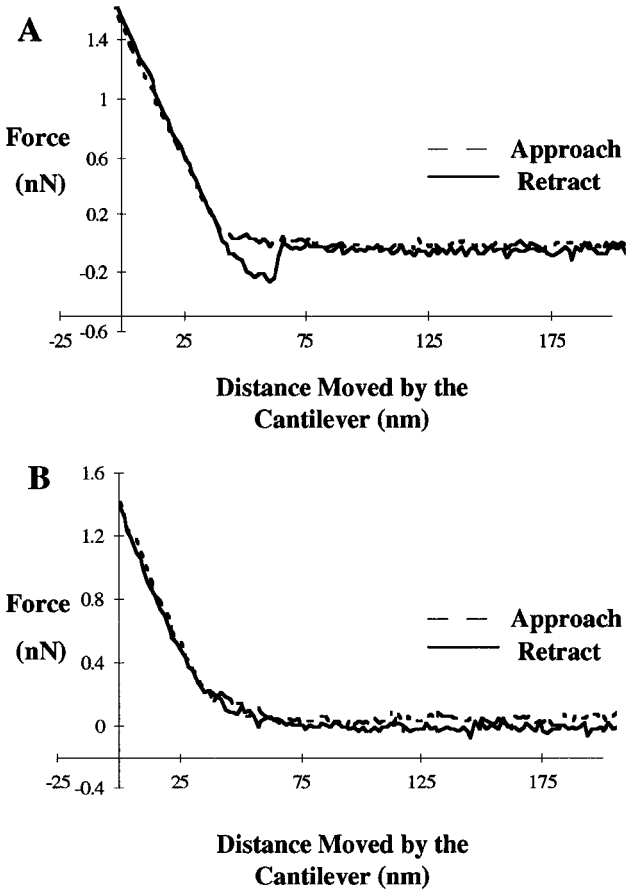

FIGURE 4: (A) Typical force measurement obtained between a ferritin-coated probe and an anti-ferritin antibody-coated silicon wafer. (B) Force measurement obtained after flooding the experimental system with excess antigen. Adhesive forces were no longer observed in such force measurements.

In all cases, force measurements were repeatable when measured at the same point on the sample surface, indicating that molecules were not being pulled off the surfaces of the probe or the substrate and also that there was minimal sample drift. A sequence of four consecutive measurements obtained at one particular point is displayed in Figure 5. In this case the force measurements are of similar overall appearance and display adhesional forces of the same magnitude. Typically, sets of at least seven to eight force curves, such as those in Figure 5, could be obtained at a single sample point before the specific interaction site was lost due to thermal drift.

To determine the force required to separate a single antigen−antibody interaction, the distribution of the adhesive forces obtained over a series of experiments was analyzed. Figure 6 displays the distribution of specific force measurements ($n = 140$), obtained with three different functionalized AFM probes, in which each data point represents a single force measurement at any position on the sample surface. The adhesive forces measured between ferritin-coated probes and anti-ferritin-coated surfaces were in the range 79−1959 pN, with the majority of the data falling between 100 and 250 pN.

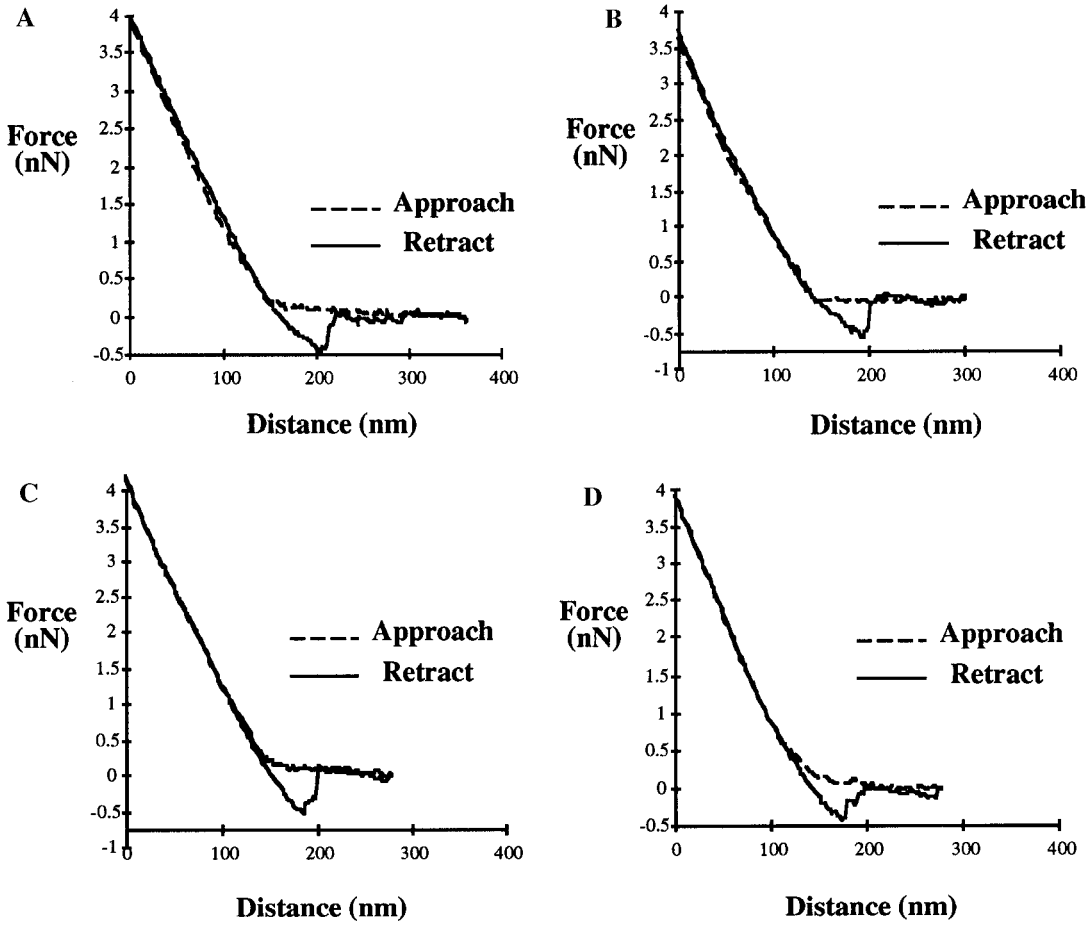

FIGURE 5: Sequence of four consecutive force measurements (A−D) obtained at a single sample point. The curves are of similar appearance and display adhesive forces of the same magnitude, illustrating the repeatability of the force measurements.

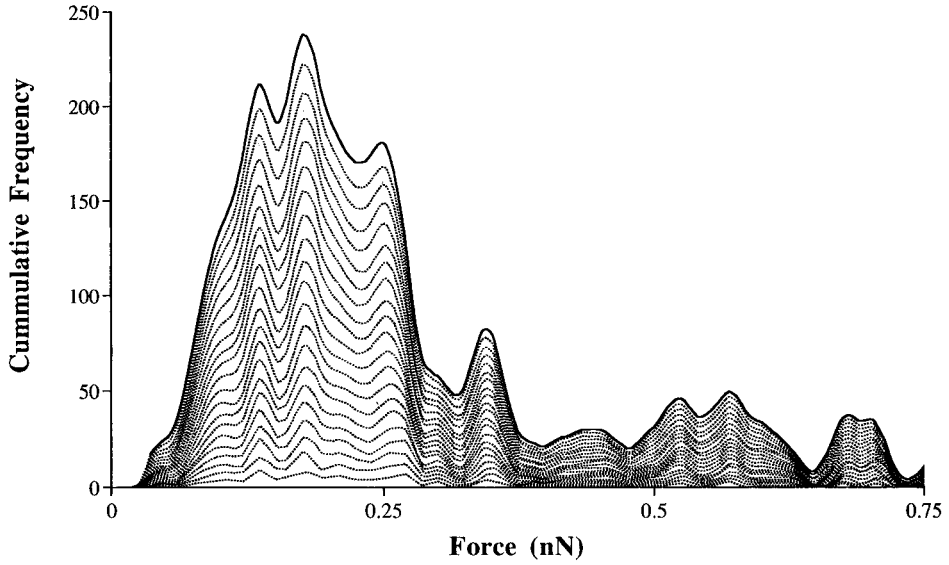

FIGURE 6: Analysis of the distribution of adhesive forces ($n = 140$) obtained with three functionalized AFM probes. Each data point represents an individual force measurement performed at any position on the sample surface. The force distribution data is plotted, using data bin sizes from 15 to 35 pN, as a stacked area graph (smallest bin size plotted lowermost). In this way, common features of the distributions are reinforced by the stacking process. A quantization in the forces, with a period of 49 ± 10 pN, is suggested by this analysis.

For small sample numbers, data frequency histograms are susceptible to the choice of data cluster or bin size. In an attempt to alleviate some of these problems, we plot the force distribution data using bin sizes from 15 to 35 pN as a stacked area graph. In this way, common features of the distributions are reinforced by the stacking process. Figure 6 suggests quantized forces, with a period of 49 ± 10 pN, which is of the same order as the 60 pN value quoted by Dammer et al. (1996), recorded for the interaction between anti-biotin antibody and biotin.

Caution, however, must always be placed when interpreting such frequency data, especially on the relatively low sample numbers used here. Values specified in the literature for similar experiments between antigens and IgG antibodies

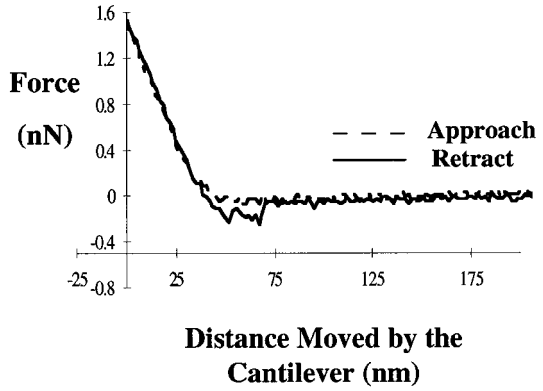

FIGURE 7: Force measurement displaying double adhesion points. Such measurements indicate the unbinding of two specific interactions.

range from 60 to 244 pN (Dammer et al., 1996; Hinterdorfer et al., 1996; Stuart et al., 1995). Dammer et al. (1996) calculated that typical antigen−antibody complexes with affinity constants ranging from 10^2 to 10^{10} M^{-1} require separation forces of 35−135 pN. The periodic force of 49 ± 10 pN observed in these experiments falls within this range and therefore may be attributed to single unbinding events between individual antigen and antibody molecules.

If this is the case, force measurements with adhesive forces larger than the above value must correspond to the separation of multiple antigen−antibody molecular pairs. For example, an adhesive force of 750 pN would represent the rupture of 15 such interactions. With an antibody molecule diameter of approximately 15 nm (Dammer et al., 1996) this would correspond to a probe-surface contact area of radius 30 nm, assuming maximum molecular packing. Such a contact area is within the range expected for most AFM probes, which are manufactured with tips of 10−50 nm radius of curvature (Thundat et al, 1992).

Analysis of the force distribution data indicated that for one of the three functionalized probes the adhesive forces tended toward larger values, implying that this particular probe produced relatively large areas of contact and/or had more ferritin molecules available for interaction. However, it can be seen from the distribution of all of the forces recorded (Figure 6) that those corresponding to two to five molecular interactions predominate, illustrating that the probe−sample contact areas in most of the measurements were sufficiently small to allow only a few specific interactions.

During these experiments it was observed that a number of the "larger" force measurements displayed multiple adhesion points. Approximately 7% of all measurements contained two adhesion points (see Figure 7), and 3% of measurements displayed three or more points of adhesion. Less than 1% of force measurements displayed no adhesion points. The immobilization strategy employed in these experiments links the antibody to the surface via amine groups present in the lysine residues of the protein molecule. Because the F_c region of the antibody molecule is relatively lysine rich there may be some preferential orientation of the antibody molecule, so that the availability of antigen-binding sites is increased. The polyepitopic nature of the antigen employed in these experiments could also increase the occurrence of binding events in force measurements.

Force curves with double adhesion points indicate that during the retract trace of the measurement cycle, two

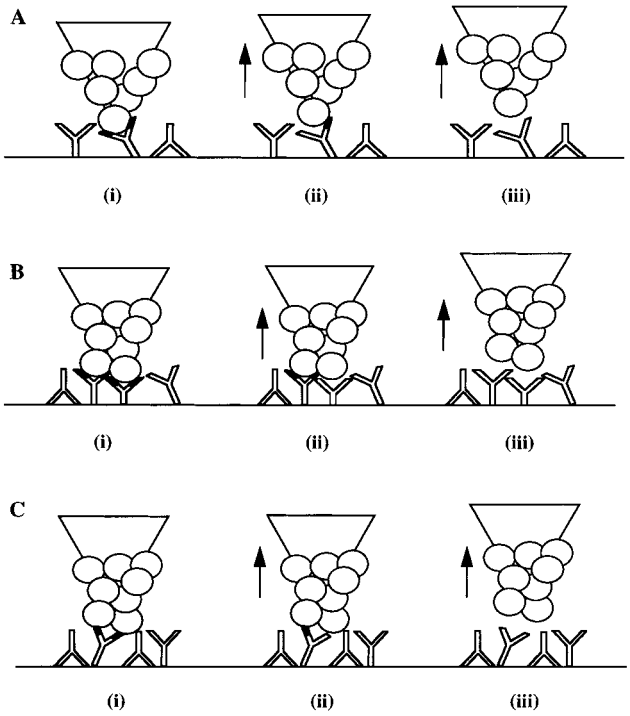

FIGURE 8: Double adhesion minima (see Figure 7) could originate in (A) the sequential unbinding of the Fab arms of the antibody from one molecule of ferritin, (B) the separate unbinding of two anti-ferritin−ferritin pairs, or (C) the sequential unbinding of the Fab arms from two molecules of ferritin. However, there are probably many more unbinding scenarios which could produce the same result. The shaded sections of the antibody molecules indicate regions still bound to the antigen, and in all cases the steps i−iii refer to (i) the bound state, (ii) after one unbinding event, and (iii) after two unbinding events. It must be noted that the sizes of the proteins and the AFM probe in this schematic are not to scale.

interactions are broken. Similar observations have recently been reported by Hinterdorfer et al. (1996). They proposed that the double adhesion minima were attributable to the interaction of one antibody molecule with one molecule of HSA, with the adhesion points arising from the unbinding of each of the Fab arms of the antibody from two separate HSA binding sites. In their experiments, the asymmetrical attachment of the PEG linker molecule to the antibody caused the separation in the observed unbinding events. Force measurements between antibodies and antigens displaying multiple adhesion points have also been detected by Dammer et al. (1996). They commented that the quantized steps observed in such force curves could correspond to the unbinding of individual antigen−antibody pairs.

It is possible that the double adhesion minima observed in our experiments originate in the sequential unbinding of the Fab arms of one antibody molecule, or neighboring antibody molecules, from a single molecule of ferritin. They could also correspond to the unbinding of two ferritin, anti-ferritin pairs, i.e., two molecules of ferritin unbinding from two antibody molecules. However, we believe an accurate estimate of the number of interacting molecules is at present problematic, since protein surface coverage of the probe can vary and the exact contact area between probe and sample, although small, is also relatively poorly characterized. For this reason, and the polyepitopic nature of ferritin, there are many different unbinding scenarios for this model antibody−antigen interaction, some of which are displayed in Figure 8.

However, the interpretation of the detailed shape of force curves may not be so straightforward. The multi-adhesion minima observed in force experiments could represent a convolution of multiple unbinding processes, including nonspecific background forces. There is also some lateral movement of the functionalized probe during force measurements. For the vertical distances moved while the probe is in contact with the sample, however, the lateral distances are only of the order of a few nanometers, and the covalent attachment of proteins should prevent a lateral displacement of the molecules on the sample surface. Nonetheless, the lateral displacement of the probe may complicate the interpretation of force curves and will remain problematic until such an effect can be compensated for.

In conclusion the data presented in this paper illustrates that it is possible to study the interactions between antibodies and antigens employed in immunoassay systems. Such experiments may also provide information relating to the manner in which the antibody molecule binds to its specific antigen, where structural or thermodynamic data may be lacking. For example, little is known about how the ferritin molecules are bound to the antibodies studied in this paper. Recently it has been shown that it is possible to produce two-dimensional maps of adhesion sites on a substrate surface (Radmacher et al., 1994 a,b). We are currently investigating the use of functionalized probes to map interaction sites on immunoassay surfaces. It is clear, therefore, that this technique has the potential to be employed as a tool to study the spatial distribution and interactions between the biomolecules in real sensor systems.

ACKNOWLEDGMENT

The authors thank C. D. Melia and P. Marshall for their assistance with the confocal microscopy and for the use of the instrument. S.A. gratefully acknowledges M. S. Hartshorne for assistance with XPS analysis.

REFERENCES

Allen, S., Davies, J., Davies, M. C., Dawkes, A. C., Edwards, J. C., Parker, M. C., Roberts, C. J., Sefton, J., Tendler, S. J. B., & Williams, P. M. (1996) *FEBS Lett. 390*, 161−164.

Binnig, G., Quate, C. F., & Gerber, C. (1986) *Phys. Rev. Lett. 56*, 930−933.

Boland, T., & Ratner, B. D. (1995) *Proc. Natl. Acad. Sci. U.S.A. 92*, 5297−5301.

Braden, C. B., & Poljak, R. J. (1995) *FASEB J. 9*, 9−16.

Bruggeman, Y. E., Schoenmakers, R. G., Schots, A., Pap, E. H. W., VanHoek, A., Visser, A. J. W. G., & Hilhorst, R. (1995) *Eur. J. Biochem. 234*, 245−250.

Butt, H. J., Jaschke, M., & Ducker, W. (1995) *Bioelectrochem. Bioenerg. 38*, 191−201.

Chu, K. S., Jin, G., Guo, J. R., Ju, M., & Huang, J. J. (1995) *Biotechnol. Prog. 11*, 352−356.

Cleveland, J. P., Manne, S., Bocek, D., & Hansma, P. K. (1993) *Rev. Sci. Instrum. 64*, 403−405.

Dammer, U., Popescu, O., Wagner, P., Anselmetti, D., Güntherodt, H.-J., & Misevic, G. (1995) *Science 267*, 1173−1175.

Dammer, U., Hegner, M., Anselmetti, D., Wagner, P., Dreier, M., Huber, W., & Güntherodt, H.-J. (1996) *Biophys. J. 70*, 2437−2441.

Davies, J., Roberts, C. J., Dawkes, A. C., Sefton, J., Edwards, J. C., Glaseby, T. O., Haymes, A. G., Davies, M. C., Jackson, D. E., Lomas, M., Shakesheff, K. M., Tendler, S. J. B., Wilkins, M. J., & Williams, P. M. (1994) *Langmuir 10*, 2654−2661.

Florin, E.-L., Moy, V. T., & Gaub, H. E. (1994) *Science 264*, 415−417.

Grubmüller, H., Heyman, B., & Tavan, P. (1996) *Science 271*, 997−999.

Hage, D. S. (1993) *Anal. Chem. 12*, R420−R424.

Harlow, E., & Lane, D. (1988a) in *Antibodies: a Laboratory Manual*, pp 27−28, Cold Spring Harbor Laboratory Press, Plainview, NY.

Harlow, E., & Lane, D. (1988b) in *Antibodies: A Laboratory Manual*, pp 553−612, Cold Spring Harbor Laboratory Press, Plainview, NY.

Harrison, P. M., & Lilley, T. H. (1989) in *Ion Carriers and Iron Proteins* (Loehr, T. M., Ed.) pp 123−229, VCH, New York.

Hinterdorfer, P., Baumgartner, W., Gruber, H. J., Schilcher, K., & Schindler, H. (1996) *Proc. Natl. Acad. Sci. U.S.A. 93*, 3477−3481.

Hoh, J. H., Cleveland, J. P., Pratter, C. B., Revel, J.-P, & Hansma, P. K. (1993) *J. Am. Chem. Soc. 114*, 4917−4919.

Hollander, Z., & Katchalski-Katzir, E. (1986) *Mol. Immunol. 23*, 927−933.

Kemeny, D. M. (1991) *A Practical Guide to ELISA*, pp 31−34, Pergamon Press, Oxford, England.

Kuo, S. C., & Lauffenburger, D. A. (1993) *Biophys. J. 65*, 2191−2200.

Leckband, D. E., Kuhl, T., Wang, H. K., Herron, J., Müller, W., & Ringsdorf, H. (1995) *Biochemistry 34*, 11467−11478.

Lee, G. U., Chrisey, L. A., & Colton, R. J. (1994a) *Science 266*, 77 −773.

Lee, G. U., Kidwell, D. A., & Colton, R. J. (1994b) *Langmiur 10*, 354−357.

Leibert, R. B., & Preive, D. C. (1995) *Biophys. J. 69*, 66−73.

Ludwig, M., Moy, V. T., Rief, M., Florin, E.-L., & Gaub, H. E. (1994) *Microsc. Microanal. Microstruct. 5*, 321−328.

Moy, V. T., Florin, E.-L., & Gaub, H. E. (1994a) *Colloids Surf. A 93*, 343−348.

Moy, V. T., Florin, E.-L., & Gaub, H. E. (1994b) *Science 266*, 257−259.

Pellequer, J. L., & Vanregenmortel, M. H. V. (1993) *J. Immunol. Methods 166*, 133−143.

Radmacher, M., Cleveland, J. P., Fritz, M., Hansma, H. G., & Hansma, P. K. (1994a) *Biophys. J. 66*, 2159−2165.

Radmacher, M., Fritz, M., Cleveland, J. P., Walters, D. A., & Hansma, P. K. (1994b) *Langmuir 10*, 3809−3814.

Roberts, C. J., Davies, M. C., Tendler, S. J. B., Williams, P. M., Davies, J., Dawkes, A. C., Yearwood, G. D. L., & Edwards, J. C. (1996) *Ultramicroscopy 62*, 149−155.

Roberts, C. J., Williams, P. M., Davies, J., Dawkes, A. C., Sefton, J., Edwards, J. C., Haymes, A. G., Bestwick, C., Davies, M. C., & Tendler, S. J. B. (1995) *Langmuir 11*, 1822−1826.

Shotton, D. (1993) in *Electronic Light Microscopy: Techniques in Modern Biomedical Microscopy*, pp 18−38, Wiley-Liss, Inc., New York.

Stuart, J. K., & Hlady, V. (1995) *Langmuir 11*, 1368−1374.

Thundat, T., Allison, D. P., Warmack, R. J., Brown, G. B., Jacobson, K. B., Schrick, J. J., & Ferrell, T. L. (1992) *Scanning Microsc. 6*, 903−910.

Vinckier, A., Heyvaert, I., D'Hoore, A., McKittrick, T., Van Haesendonck, C., Engelborghs, Y., & Hellemans, L. (1995) *Ultramicroscopy 57*, 337−343.

Williams, P. M., Davies, M. C., Jackson, D. E., Roberts, C. J., Tendler, S. J. B., & Wilkins, M. J. (1991) *Nanotechnology 2*, 172−181.

BI962531Z